# *Highly effective nanoparticle removal in plant-based water filters*

Laxmicharan Samineni[1, *], Sophie DeRespino[2], Mekayla Depaolis[2], Rashmi P Mohanty[3], Yu-Ming Tu[1], Stephanie Velegol[4], Debadyuti Ghosh[3], Manish Kumar[2, *]

[1]McKetta Department of Chemical Engineering, University of Texas at Austin, Austin, Texas, 78712, United States

[2]Department of Civil, Architectural and Environmental Engineering, University of Texas at Austin, Austin, Texas, 78712, United States

[3]Division of Molecular Pharmaceutics and Drug Delivery, College of Pharmacy, The University of Texas at Austin, Austin, Texas, 78712, United States

[4]Department of Chemical Engineering, The Pennsylvania State University, University Park, Pennsylvania, 16802, United States

[*]Corresponding author

**Materials and Methods**

**Natural fibers:** The cotton fiber used in this study as a filter substrate was purchased from a local Walmart store (Equate Beauty Jumbo Cotton Balls, 400 Count). They are easily accessible and the link to their purchase is as follows.

Cotton: https://www.walmart.com/ip/Equate-Beauty-Jumbo-Cotton-Balls-400-Count/280043267

**Quantification of T7 bacteriophage removal**: Standard filtration experiments similar to that used to quantify the nanoparticle removal efficiency were used for the quantification of the T7 bacteriophage. After preparing a *MO*-functionalized filter according to the procedure in the prior section, the filter was equilibrated with 100mL of 1mM NaCl solution at the required flowrate for the filtration experiment. After equilibration, the influent solution containing ~$10^8$PFU/mL of T7 bacteriophage dispersed in 1mM NaCl was passed through the *MO*-functionalized cotton filter at 2mL/min. Note that the main difference between the experiments is that the effluent samples for T7 bacteriophage were collected as fractions of 1mL when 50mL, 75mL, and 100mL of the influent has passed through the filter. Experimental log removal efficiency (LRE) of the filters was quantified using **Eqn. 1** after quantifying the concentration of viable pathogens in influent and effluent samples using a double-layer plaque assay (1).

**T7 propagation:** T7 bacteriophage is a lytic bacterial virus that infects and propagates in *E. coli*. We used the BL21 host strain procured from Millipore Sigma for the propagation. A single colony of the BL21 bacteria was grown in M9LB media (Thermo Fischer Scientific) while shaking at 250rpm overnight at 37°C. The next morning, the fresh overnight culture was inoculated in an M9LB medium at a dilution of 1:100 and incubated while shaking at 250rpm and 37°C. Once the optical density ($OD_{600}$) reached 0.2-0.3 (early logarithmic growth phase), we infected the culture with T7 phage at a multiplicity of infection (MOI) of 0.001-0.01 and continued the

shaking at 37°C for 1-3h until lysis is observed based on the transparency of the culture. After lysis occurs, NaCl was added to a final concentration of 0.5M to lyse the remaining bacteria, which is then clarified by spinning at 10,000rpm at 4°C for 20min. The remaining supernatant is then purified following two steps of PEG purification. In the first step, 1/6 volume of 50% PEG-8000 was added to the remaining supernatant, which was left on ice for at least 30min to precipitate the phage particles. The lysate-PEG mixture was then centrifuged for 30min at 14,000rpm. The pellet formed was resuspended with 1mL of 1X PBS for the second purification step. The mixture was then transferred to a fresh microcentrifuge tube, and 200µL of 50% PEG-8000 was added and allowed to stand on ice for at least 30min for phage precipitation. Next, the lysate-PEG mixture was centrifuged for 30min at 14,000rpm to collect the phage particles in the pellet. The pellet was then resuspended in 100µL 1X PBS and stored at 4°C until ready to use.

**T7 quantification:** We performed the standard double layer plaque assay to quantify the influent and effluent phage titers. Similar to the T7 propagation step, BL21 overnight host culture was inoculated in M9LB medium at 1:100 dilution and incubated while shaking at 37°C to an optical density ($OD_{600}$) of 1.0 (stationary growth phase). A sufficient volume of top agarose was melted and then maintained at 55°C. For at least one hour, the desired number of LB-agar plates were warmed to 37°C until ready for use. Samples to be quantified were diluted using 10-fold serial dilutions of phage in 1X PBS. A series of tubes were prepared by pipetting 200µL of host cells into the tubes. The host cells were infected with 10µL of the phage dilutions in each tube. Then, 1.5mL agarose top was added to each phage infected tube, vortex mixed, and the content was poured onto one well of a pre-warmed LB agar 6-well plates. The plate was allowed to sit temporarily until the top agarose hardens, then inverted and incubated for 3-4h at 37°C or overnight at room temperature to allow the plaque formation. The plaques were counted and quantified based on the dilution factor.

**SDS-PAGE gel electrophoresis and Mass spectrometry**: To qualitatively analyze the Moringa proteins adsorbed on the surface of the cotton, the standard SDS-PAGE gel electrophoresis technique was used. The proteins adsorbed on the cotton were first desorbed into a 600mM NaCl solution by flowing 100mL of salt solution through a Moringa functionalized cotton column. The protein solution was then run through a ready-made NuPAGE Novex 4-12% Bis-Tis gel with MOPS (3-(N-morpholino) propanesulfonic acid) buffer. Novex Sharp pre-stained standard was used as the protein ladder for molecular weight determination of the Moringa proteins. Standard Coomassie staining and destaining protocols were used to visualize the protein bands. Individual protein bands cut from the resultant gel were digested using trypsin and subjected to mass spectrometry at the Proteomics Facility, the University of Texas at Austin.
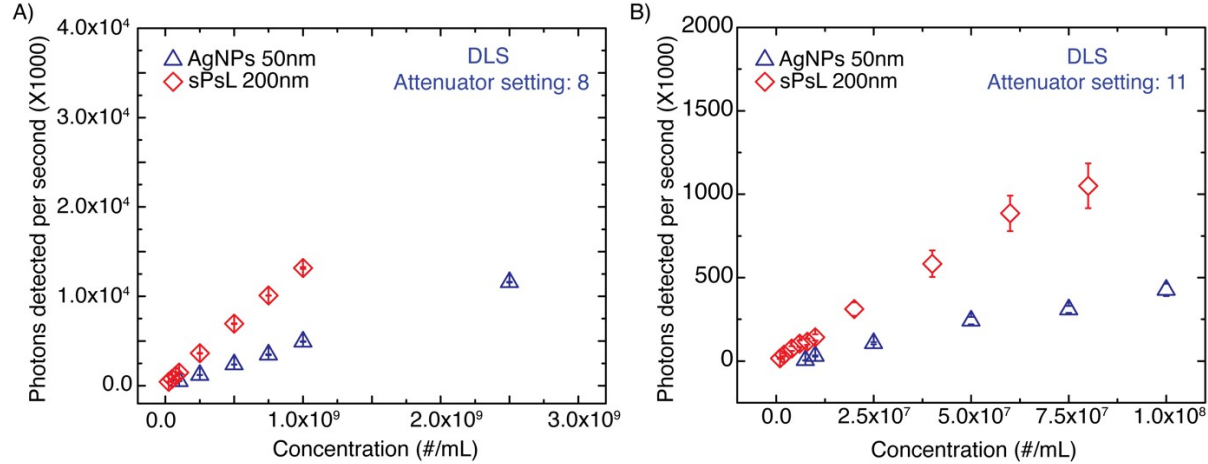
**Figure S1. Two calibration curves were developed for the analysis of 200nm polystyrene latex (sPsL) particles and 50nm silver nanoparticles (AgNPs) using Dynamic light scattering (DLS) to measure the concentration of influent and effluent samples from the filtration experiments A)** Calibration curves were developed at an attenuator level of 8 for the quantification of samples with high nanoparticle concentration. The samples prepared for the high concentration calibration curve cover the range of $2.5 \times 10^7$#/mL to $1.0 \times 10^9$#/mL and $1.0 \times 10^8$#/mL to $2.5 \times 10^9$#/mL for the sPsL particles and the AgNPs respectively. The calibration curves developed for high concentration samples were used to quantify the influent samples and effluent samples from unfunctionalized cotton filters **B)** Calibration curves were developed at an attenuator level of 11 for the quantification of samples with low nanoparticle concentration. The samples prepared for the high concentration calibration curve cover the range of $1.0 \times 10^6$#/mL to $8.0 \times 10^7$#/mL and $7.5 \times 10^6$#/mL to $1.0 \times 10^8$#/mL for the sPsL particles and the AgNPs respectively. The calibration curves developed for low concentration samples were used to quantify the effluent sample concentration from *MO*-functionalized cotton filters. Three measurements were made for each sample at a fixed measurement position of 4.65 mm and with 11 scans per measurement.
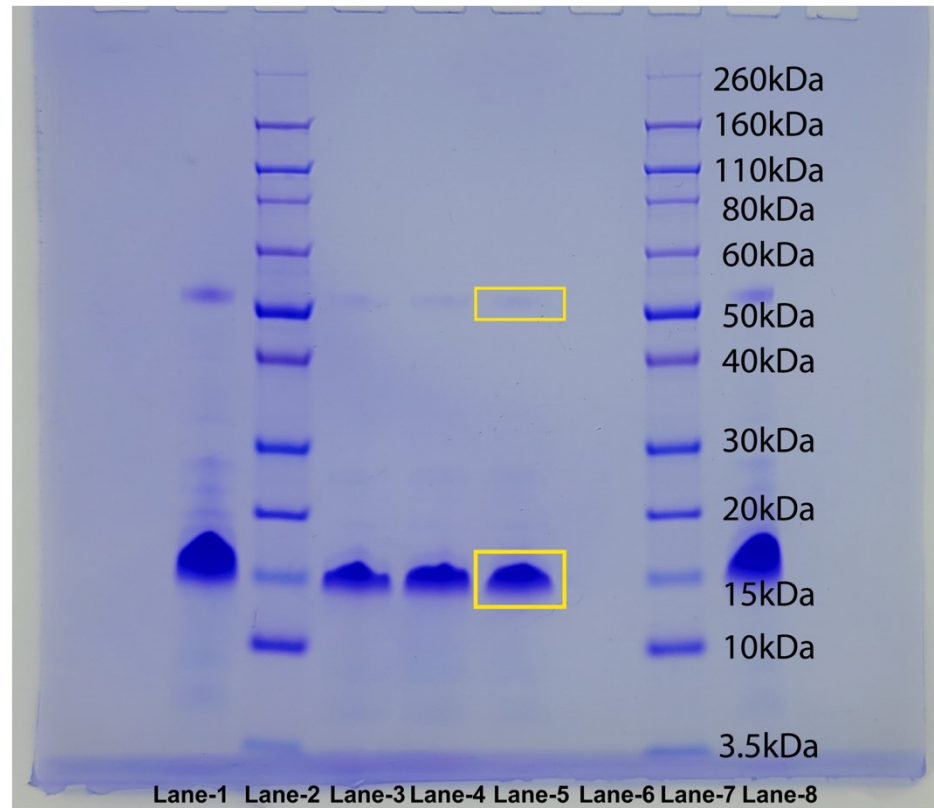
**Figure S2. SDS-PAGE gel electrophoresis and mass spectrometry show the presence of Moringa oleifera chitin binding protein (MoCBP) on the surface of Moringa functionalized cotton A)** SDS-PAGE gel electrophoresis of 600 mM NaCl eluent of the protein adsorbed on the surface of cotton using a 4-12% pre-made Bis-Tris gel. Lanes 2 and 7 show protein markers and lanes 3, 4, and 5 show the protein bands corresponding to the salt wash sample from three different Moringa functionalized cotton columns. The highlighted portions of the gel were incised and submitted for mass spectrometry analysis using trypsin digestion. The results indicate the presence of Moringa protein, MoCBP, on the surface of cotton.

**Table S1: Nanoparticle removal efficiencies reported in this study compared to literature reported values**

| Research Study | Nanoparticles tested | Removal techniques | Test water | Removals reported |
|---|---|---|---|---|
| Zhang 2008 (2) | $TiO_2$ and ZnO | Coagulation and flocculation<br>Alum dosage – 20 mg/L | Nanopure water and tap water<br>pH -7.7±0.2<br>Ionic strength - 0.01 M | 20-80% |
| Honda 2013 (3) | $TiO_2$ | Coagulation, flocculation, and sedimentation<br>$FeSO_4$ – 50 mg/L<br>$Al_2(SO_4)_3$ – 50 mg/L<br>$FeCl_3$– 50 mg/L | Artificial groundwater and Artificial surface water with ionic strengths of 0.01 M and 0.0183M; No organic matter was used in the test solution | $FeSO_4$ – >90%<br>$Al_2(SO_4)_3$ – >90%<br>$FeCl_3$ – <60% |
| Chang 2017 (4) | $TiO_2$ | Drinking water treatment including pre-chlorination, sedimentation, filtration, and chlorination | DI water<br>Changxing Riverwater<br>Fengshan Riverwater | 52.6 – 97.3% |
| Gopakumar 2017 (5) | $Fe_2O_3$ | Meldrum acid modified Cellulose nanofiber based polyvinylidene fluoride microfiltration | Buffered water solution<br>pH - 7 | Complete removal was reported based on SEM images and UV-Vis |

| | | | | |
|---|---|---|---|---|
| Chalew 2013 (6) | TiO$_2$, Ag, ZnO | Conventional removal | Ground water, Surface water, Synthetic freshwater, Synthetic fresh water with NOM, and Tertiary wastewater effluent | Lowest removal of 0.46±2.42 and highest removal of 97.9 ±1.19 |
| Chalew 2013 (6) | TiO$_2$, Ag, ZnO | Microfiltration | Ground water, Surface water, Synthetic freshwater, Synthetic fresh water with NOM, and Tertiary wastewater effluent | Lowest removal of 17.3±5.62 and highest removal of 99.6 ± 0.21 |
| Chalew 2013 (6) | TiO$_2$, Ag, ZnO | Ultrafiltration | Ground water, Surface water, Synthetic freshwater, Synthetic fresh water with NOM, and Tertiary wastewater effluent | Lowest removal of 3.93±33.0 and highest removal of 100 ± 5.09 |
| This Study | Polystyrene latex beads and Ag nanoparticles | *MO*-functionalized cotton filters | Buffered water with salt concentrations in the range of 1-20 mM and pH in the 5.5-8.5 | 99.5 – 99.999% |

**Table S2: The high sticking coefficients of sPsL particles and AgNPs in *MO*-cotton filters compared to those in unfunctionalized cotton filters represent favorable interactions between *MO* proteins and nanoparticles tested in this study.** The sticking coefficients were calculated using the well-established clean-bed filtration model for fibrous filters and the TE model (Tufenkji and Elimelech) for single collector efficiency from the literature (7, 8). Microsoft Excel spreadsheets are available in supporting files for details on the parameters and procedures used for these calculations. Note that a nominal log removal of 0.01 was used to calculate the control cotton sticking coefficient as the experimental values show negative removal which will yield unphysical values.

| Nanoparticle | Sticking coefficient (Uncoated cotton) | Sticking coefficient (*MO*-cotton) | Ratio of sticking coefficients ($\alpha_{MOcotton}/\alpha_{control}$) |
|---|---|---|---|
| 200nm sPsL particles | 7.41E-05 | 1.25E-01 | 1686.90 |
| 50nm AgNPs | 3.34E-04 | 7.52E-02 | 225.15 |

**Table S3: Protein identification results from mass spectrometry indicate the presence of MoCBP protein.** Samples 1 and 2 refer to the two incisions made on the SDS-gel shown in Figure S2. The rows with relevant proteins were highlighted for reference. Raw data in excel format is available in supporting information.

| # | Visible? | Starred? | Identified Proteins | Accession Number | Alternate ID | Molecular Weight | Protein Grouping Ambiguity | Taxonomy | Sample 1 | Sample 2 |
|---|---|---|---|---|---|---|---|---|---|---|
| 1 | TRUE | Empty | Filaggrin OS=Homo sapiens OX=9606 GN=FLG PE=1 SV=3 | Cont_P20930 | FLG | 435 kDa | | unknown | 19.801 | 25.01 |
| 2 | TRUE | Empty | Keratin, type II cytoskeletal 1 OS=Homo sapiens OX=9606 GN=KRT1 PE=1 SV=6 | Cont_P04264 | KRT1 | 66 kDa | TRUE | unknown | 9.4293 | 43.589 |
| 3 | TRUE | Empty | Filaggrin OS=Homo sapiens OX=9606 GN=FLG PE=1 SV=3 | Cont_P20930-DECOY | | ? | | unknown | 19.801 | 20.723 |
| 4 | TRUE | Empty | Keratin, type II cytoskeletal 2 epidermal OS=Homo sapiens OX=9606 GN=KRT2 PE=1 SV=2 | Cont_P35908 | KRT2 | 65 kDa | TRUE | unknown | 12.258 | 28.583 |
| **5** | **TRUE** | **Empty** | **2S albumin precursor [Moringa oleifera]** | **AHG99682.1** | | **19 kDa** | **TRUE** | **unknown** | **79.206** | **2.8583** |
| 6 | TRUE | Empty | Keratin, type I cytoskeletal 9 OS=Homo sapiens OX=9606 GN=KRT9 PE=1 SV=3 | Cont_P35527 | KRT9 | 62 kDa | TRUE | unknown | 7.5434 | 32.871 |

| 7 | TRUE | Empty | CBP3 OS=Moringa oleifera OX=3735 PE=3 SV=1 | A0A3G6IGT2 | | 19 kDa | TRUE | unknown | 59.404 | 0 |
|---|------|-------|--------------------------------------------|-------------|--|--------|------|---------|--------|---|
| 8 | TRUE | Empty | Keratin, type I cytoskeletal 10 OS=Homo sapiens OX=9606 GN=KRT10 PE=1 SV=6 | Cont_P13645 | KRT10 | 59 kDa | TRUE | unknown | 4.7146 | 22.867 |
| 9 | TRUE | Empty | Keratin, type II cytoskeletal 5 OS=Homo sapiens OX=9606 GN=KRT5 PE=1 SV=3 | Cont_P13647 | KRT5 | 62 kDa | TRUE | unknown | 13.201 | 25.725 |
| 10 | TRUE | Empty | 2S albumin precursor [Moringa oleifera] | AHG99681.1 | | 19 kDa | TRUE | unknown | 0 | 2.8583 |
| 11 | TRUE | Empty | CBP3 OS=Moringa oleifera OX=3735 PE=3 SV=1 | A0A3G6IGI3 (+1) | | 18 kDa | TRUE | unknown | 68.834 | 0 |
| 12 | TRUE | Empty | CBP3 OS=Moringa oleifera OX=3735 PE=3 SV=1 | A0A3G6IME9 | | 19 kDa | TRUE | unknown | 44.318 | 2.1437 |

**Effect of divalent cations and anions on *MO* cotton filter nanoparticle removal efficiency:** To understand the effect of divalent cation and anion presence on the nanoparticle removal efficiency of *MO* cotton filters, column experiments were conducted with $Na_2SiO_3$, $Na_2SO_4$, $MgCl_2$, and $CaCl_2$ as background buffers. 20 mM strength buffers were prepared with the individual salts and filtered through 0.22 μm membrane filters. 200 nm sPsL nanoparticles were spiked into the buffer solutions at a final concentration of $10^{10}$ #/mL. 100 mL of the resultant influent solution was filtered through *MO* cotton filters prepared according to the procedure described in the main manuscript and effluent was collected into two 50 mL fractions. The removal efficiency was calculated by quantifying the influent and 50-100 mL effluent fraction concentrations using DLS analysis. Note that a filtration flow rate of 30 mL/min was used for these experiments and column filters were equilibrated with 100 mL of background buffer before filtering the nanoparticle-spiked groundwater. The results shown in **Fig. S3** indicate that the presence of divalent anions decreased the removal efficiency of the *MO* cotton filters slightly but divalent cations showed no significant impact. The effect of individual ions on the removal mechanism needs to be studied closely in future studies.
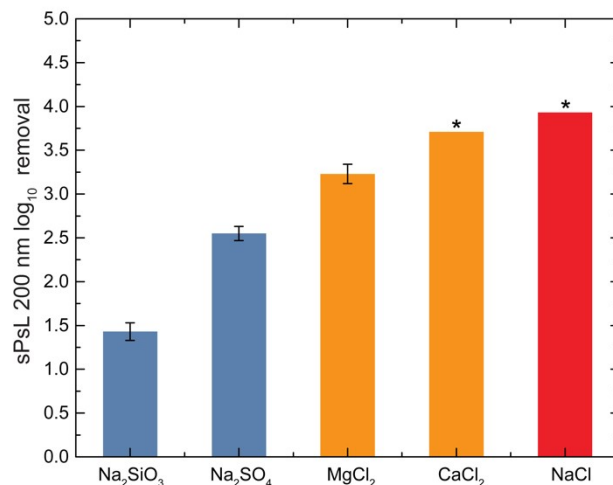
**Figure S3: *MO* cotton filters achieve significant nanoparticle removal in the presence of divalent cations and anions (Ca$^{2+}$, Mg$^{2+}$, SiO$_3^{2-}$, and SO$_4^{2-}$).** Column experiments were performed to test the removal efficiency of *MO* functionalized cotton filters against $10^{10}$ #/mL 200 nm sPsL particles spiked in 20 mM buffer solutions with Na$_2$SiO$_3$, Na$_2$SO$_4$, MgCl$_2$, and CaCl$_2$ to study the effect of the presence of divalent cations and anions. The *MO* cotton filters achieved removal efficiencies of $1.43\pm0.10$, $2.55\pm0.08$, $3.23\pm0.11$, and $>3.71$ log$_{10}$ removals respectively compared to $>4$ log$_{10}$ in the presence of monovalent ions. *Indicates that the effluent concentration was below the limit of detection which indicates that the actual removal could be higher than the reported values. Error bars represent the standard deviation from three independent measurements.

***MO* cotton filter removal efficiency against groundwater spiked with nanoparticles:** To quantify the removal efficiency of *MO* cotton filters against nanoparticles in a realistic water matrix, column experiments were conducted with groundwater samples. Two cases were tested in which 1) groundwater sample was used as is to spike the nanoparticles and 2) groundwater was filtered through a 0.22 µm membrane filter before spiking with nanoparticles. The total organic content, total dissolved solids, and pH of the groundwater were using routine analysis (**Table S4**) tested before introducing nanoparticles in both cases. Once analyzed, 200 nm sPsL nanoparticles were spiked into the water matrix at a final concentration of $10^{10}$ #/mL. 100 mL of the resultant influent solution was filtered through *MO* cotton filters prepared according to the procedure described in the main manuscript and effluent was collected into two 50 mL fractions. The removal efficiency was calculated by quantifying the influent and 50-100 mL effluent fraction concentrations using DLS analysis. Note that a filtration flow rate of 30 mL/min was used for these experiments and column filters were equilibrated with 100 mL of DI water before filtering the nanoparticle-spiked groundwater. The results shown in **Fig. S4** indicate that the presence of groundwater matrix does not show any significant effect on the removal efficiency of *MO* cotton filters.
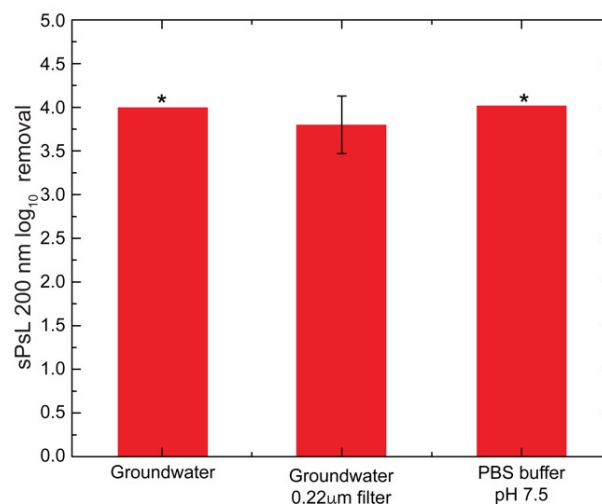
**Figure S4: No significant impact was observed on the nanoparticle removal efficiency of *MO-cotton* filters when groundwater was used as a background matrix.** Experimental $\log_{10}$ removal of sPsL particles spiked at a concentration of $10^{10}$ #/mL in groundwater samples using *MO*-functionalized cotton filters at a flow rate of 30 mL/min showed that *MO*-cotton filters achieve high removal of sPsL particles. No significant change in the removal efficiency was found compared to the experiments conducted with phosphate-buffered saline as a background buffer. *Indicates that the effluent concentration was below the limit of detection which indicates that the actual removal could be higher than the reported values. Error bars represent the standard deviation from three independent measurements.

| Sample | Total Organic Content (mg/L) | Total Dissolved Solids (ppm) | pH |
|---|---|---|---|
| Groundwater | 2.21±0.43 | 680.47±12.16 | 8.12 |
| Groundwater filtered (0.22 μm filtered) | 1.84±0.07 | 442.22±1.93 | 8.51 |

**Table S4**: TOC, TDS, and pH analysis of the groundwater sample before and after filtration with 0.22 um membrane filter used as a background for experiments shown in **Figure S4**.

**References:**

1.      Adams MH. Bacteriophages: Citeseer; 1959.
2.      Zhang Y, Chen Y, Westerhoff P, Hristovski K, Crittenden JC. Stability of commercial metal oxide nanoparticles in water. Water research. 2008;42(8-9):2204-12.
3.      Honda RJ, Keene V, Daniels L, Walker SL. Removal of TiO2 nanoparticles during primary water treatment: Role of coagulant type, dose, and nanoparticle concentration. Environmental engineering science. 2014;31(3):127-34.
4.      Chang H-H, Cheng T-J, Huang C-P, Wang G-S. Characterization of titanium dioxide nanoparticle removal in simulated drinking water treatment processes. Science of the Total Environment. 2017;601:886-94.
5.      Gopakumar DA, Pasquini D, Henrique MA, de Morais LC, Grohens Y, Thomas S. Meldrum's Acid Modified Cellulose Nanofiber-Based Polyvinylidene Fluoride Microfiltration Membrane for Dye Water Treatment and Nanoparticle Removal. ACS Sustainable Chemistry & Engineering. 2017;5(2):2026-33.
6.      Chalew TEA, Ajmani GS, Huang H, Schwab KJ. Evaluating nanoparticle breakthrough during drinking water treatment. Environmental health perspectives. 2013;121(10):1161-6.
7.      Logan BE, Hilbert TA, Arnold RG. Removal of bacteria in laboratory filters: models and experiments. Water Res. 1993;27(6):955-62.
8.      Tufenkji N, Elimelech M. Correlation equation for predicting single-collector efficiency in physicochemical filtration in saturated porous media. Environ Sci Technol. 2004;38(2):529-36.